A Manganese Single-Chain Magnet Exhibits a Large Magnetic Coercivity

Chen-I Yang,[a,b] **Yu-Jhe Tsai,**[a] **Shao-Po Hung,**[a] **Hui-Lien Tsai,**[*a] **Motohiro Nakano**[*c]

[a]Department of Chemistry, National Cheng Kung University, Tainan, Taiwan 70101, R. O. C.

[b]Institute of Chemistry, Academia Sinica, Taipei 115, Taiwan, R. O. C.

[c]Division of Applied Chemistry, Graduate School of Engineering, Osaka University, 2-1 Yamada-oka, Suita, 565-0871, Japan

Experimental section

Synthesis. All solvents and reagents were used as received, (no purification was necessary). All reactions were performed under aerobic conditions.

Safety note: Azide salts are potentially explosive; such compounds should be synthesized and used in small quantities and treated with the utmost care at all times.

[Mn$_6$O$_2$(4-MeOsalox)$_6$(N$_3$)$_2$(MeOH)$_4$]$_n$. Mn(NO$_3$)$_2$·4H$_2$O (0.253 g, 1.00 mmol) and sodium azide (0.0648 g, 1.00 mmol) were dissolved in MeOH (60 mL). 4-MeO-H$_2$salox (0.167 g, 1.00 mmol) and 10 wt% water solution of NEt$_4$OH (1.428 g, 0.97 mmol) were added to this solution, resulting in a deep brown solution which was stirred for 10 min. The resulting solution was filtered.   The filtrate was undisturbed to give deep brown crystals of **1** (yield 40%). Elemental Analysis (%) calcd for C$_{52}$H$_{58}$Mn$_6$N$_{12}$O$_{24}$: C 39.92, H 3.74, N 10.74; found: C 39.37, H 3.86, N 10.70; selected IR data (KBr disk, cm^{-1}): 3408 (m), 3004 (w), 2943 (w), 2084 (s), 1605 (vs), 1584 (vs), 1533 (s), 1488 (m), 1439 (m), 1414 (m), 1354 (w), 1292 (w), 1232 (vs), 1216 (vs), 1168 (s), 1147 (m), 1126 (m), 1027 (vs), 976 (m), 833 (w), 813 (w), 789 (w), 749 (m), 667 (s), 643 (s), 591 (w), 463 (m)

X-ray Crystallography. Diffraction measurements for complex **1** were carried out using a Brucker SMART APEXII CCD diffractometer with graphite-monochromated Mo Kα radiation (λ = 0.7107 Å). Data collection parameters of **1** are listed in Table S1. Structure was solved using direct methods and refined using the SHELXL-97[1] program by full-matrix least-squares on F^2 values. All non-hydrogen atoms were refined anisotropically, whereas the hydrogen atoms were placed in ideal, calculated positions, with isotropic thermal parameters riding on their respective carbon atoms.

Magnetic measurement. Variable temperature DC and AC magnetic susceptibilities were

2

collected for microcrystalline samples, restrained in eicosane to prevent torquing, on a Quantum Design MPMS-XL SQUID magnetometer equipped with a 7.0 Tesla magnet and operating in the range of 1.8 – 300.0 K. Hysteresis loops were performed on an aligned-crystals sample using a Quantum Design MPMS SQUID VSM magnetometer in continuous measurement mode. Diamagnetic corrections were estimated from Pascal's constants[2] and subtracted from the experimental susceptibility data to obtain the molar paramagnetic susceptibility of the compounds. Measurements of the heat capacity for a grounded polycrystalline sample (pellet piece) of complex **1** between T = 2.1 K and T = 150 K were made with a Quantum Design PPMS instrument using a hybrid adiabatic relaxation method. The two-tau relaxation method was used with PPMS software to determine the heat capacity.

Other Studies. Infrared spectra were recorded in the solid state (KBr pellets) on a Nicolet Magna 550 FTIR spectrometer in the 400-4000 cm^{-1} range. Elemental analyses were carried out by using an Elementar vario EL III analyzer.

1. G. M. Sheldrick, *SHELXL-97*; University of Gottingen: Gottingen, Germany, **1997**.

2. E. A. Boudreaux, L. N. Mulay, *Theory and Applications of Molecular Paramagnetism*, Wiley J. & Sons, New York, **1976**; p. 491.

Table 1S. Crystallographic data for complex **1**

	1
Empirical formula	$C_{52}H_{58}Mn_6N_{12}O_{24}$
Formula weight	1564.74
Temperature	150(2) K
Wavelength	0.71073 Å
Crystal system	Monoclinic
Space group	$P2_1/c$
Unit cell dimensions	a = 10.0446(5) Å
	b = 22.3020(12) Å β = 90.1650(10)°
	c = 13.3085(7) Å
Volume	2981.3(3) Å^3
Z	2
Density (calculated)	1.743 Mg/m^3
Absorption coefficient	1.326 mm^{-1}
F(000)	1592
Crystal size	$0.40 \times 0.12 \times 0.10$ mm^3
Theta range for data collection	1.78 to 28.36°.
Index ranges	$-9 \leq h \leq 13, -29 \leq k \leq 29, -17 \leq l \leq 17$
Reflections collected	23088
Independent reflections	7440 [R(int) = 0.0183]
Completeness to theta =25.00°	99.8 %
Absorption correction	Multi-scan
Refinement method	Full-matrix least-squares on F^2
Data / restraints / parameters	7440 / 0 / 422
Goodness-of-fit on F^2	1.048
Final R indices [I>2sigma(I)]	$R1^a$ = 0.0321, $wR2^b$ = 0.0837
R indices (all data)	$R1$ = 0.0362, $wR2$ = 0.0863
Largest diff. peak and hole	1.489 and -1.329 e.Å^{-3}

$^aR1 = (\Sigma||F_O|-|F_C||)/\Sigma|F_O|$ $^bwR2 = [\Sigma[w(F_O{}^2-F_C{}^2)^2]/\Sigma[w(F_O{}^2)^2]]^{1/2}$

Table 2S. Bond valence sums[3,4] calculated for manganese centers for complex **1**.

	Complex **1**		
	Mn1	Mn2	Mn3
Mn(II)	3.40	3.38	3.45
Mn(III)	*3.18*	*3.15*	*3.23*
Mn(IV)	3.10	3.08	3.15

3. W. Liu, H. H. Thorp, *Inorg. Chem.* **1993**, *32*, 4102-4105.

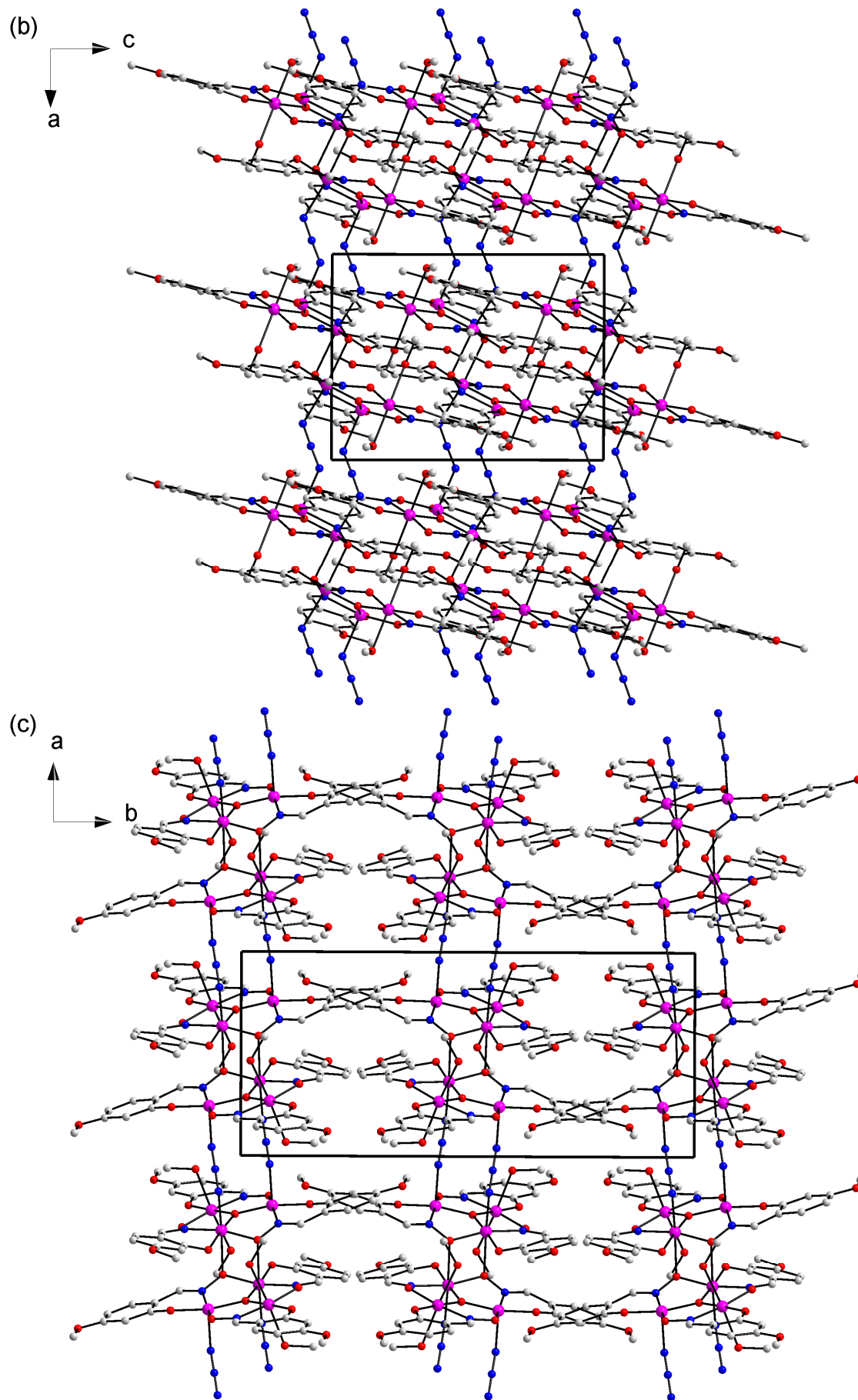4. I. D. Brown, D. Altermatt, *Acta Crystallogr*. Sect. B **1985**, 41, 244-247.

(a)

(b)

(c)
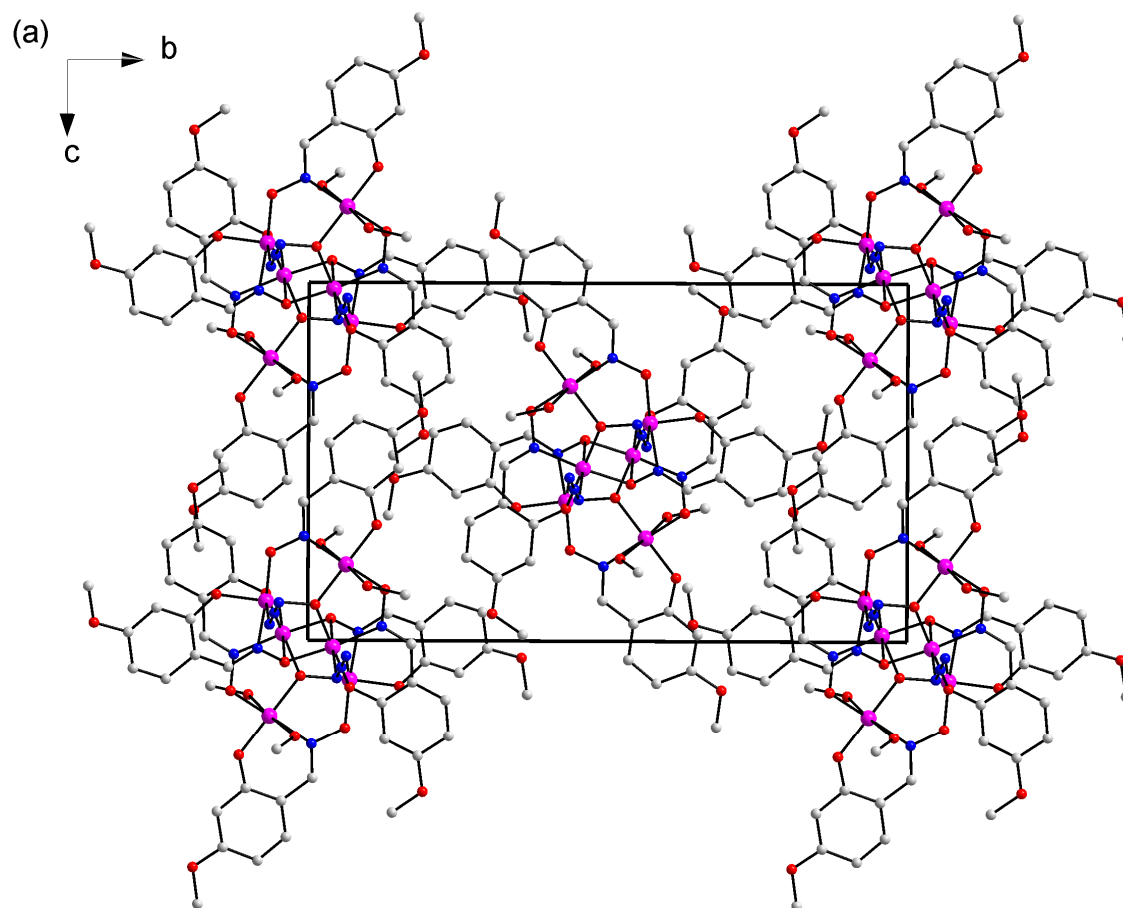
Figure 1S. View of the packing arrangement of complex **1** along *a* axis (a), *b* axis (b), and *c* axis (c).
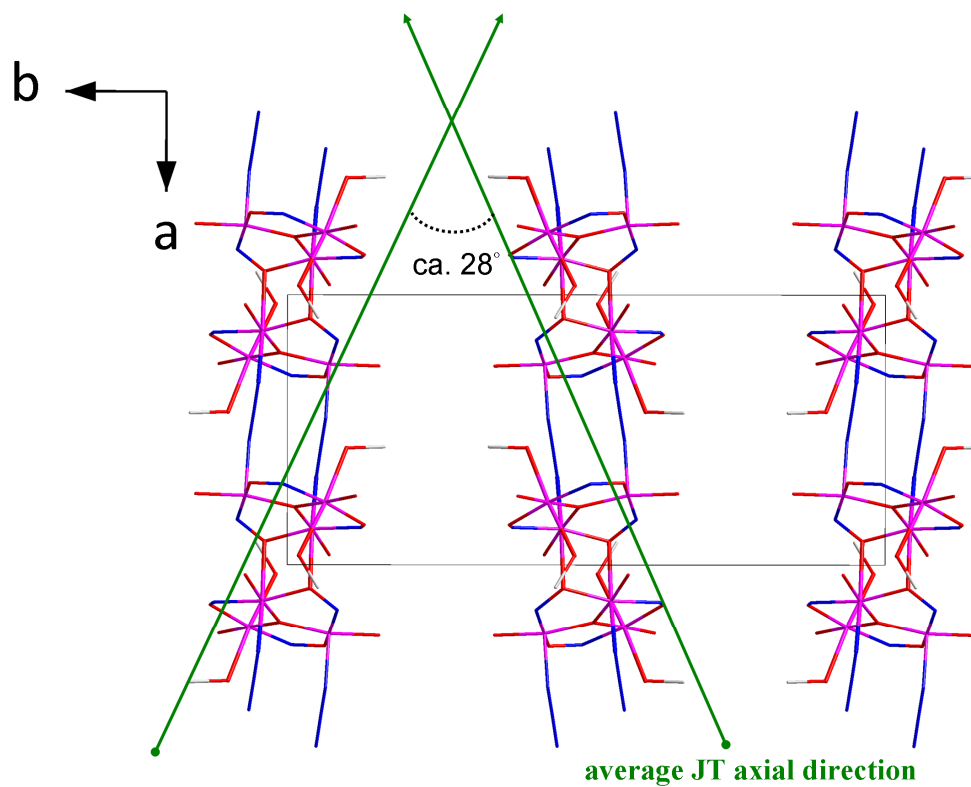

Figure 2S. Angle of the average JT axial directions for various symmetrical chains.
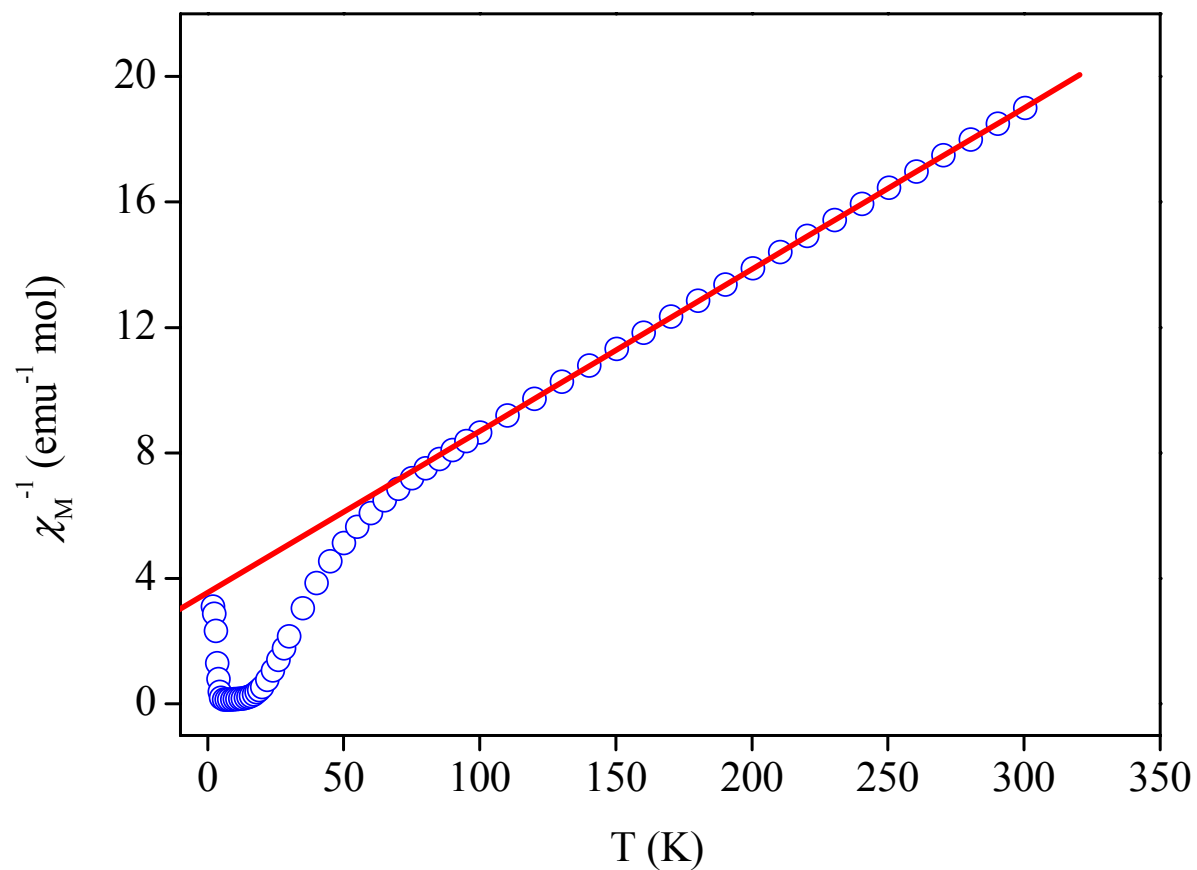
Figure 3S. Plot of χ_M^{-1} ($\circ$) vs. temperature for a microcrystalline sample of complex **1**. The solid line represents the best fit of χ_M^{-1} above 100 K with a Curie-Weiss law.
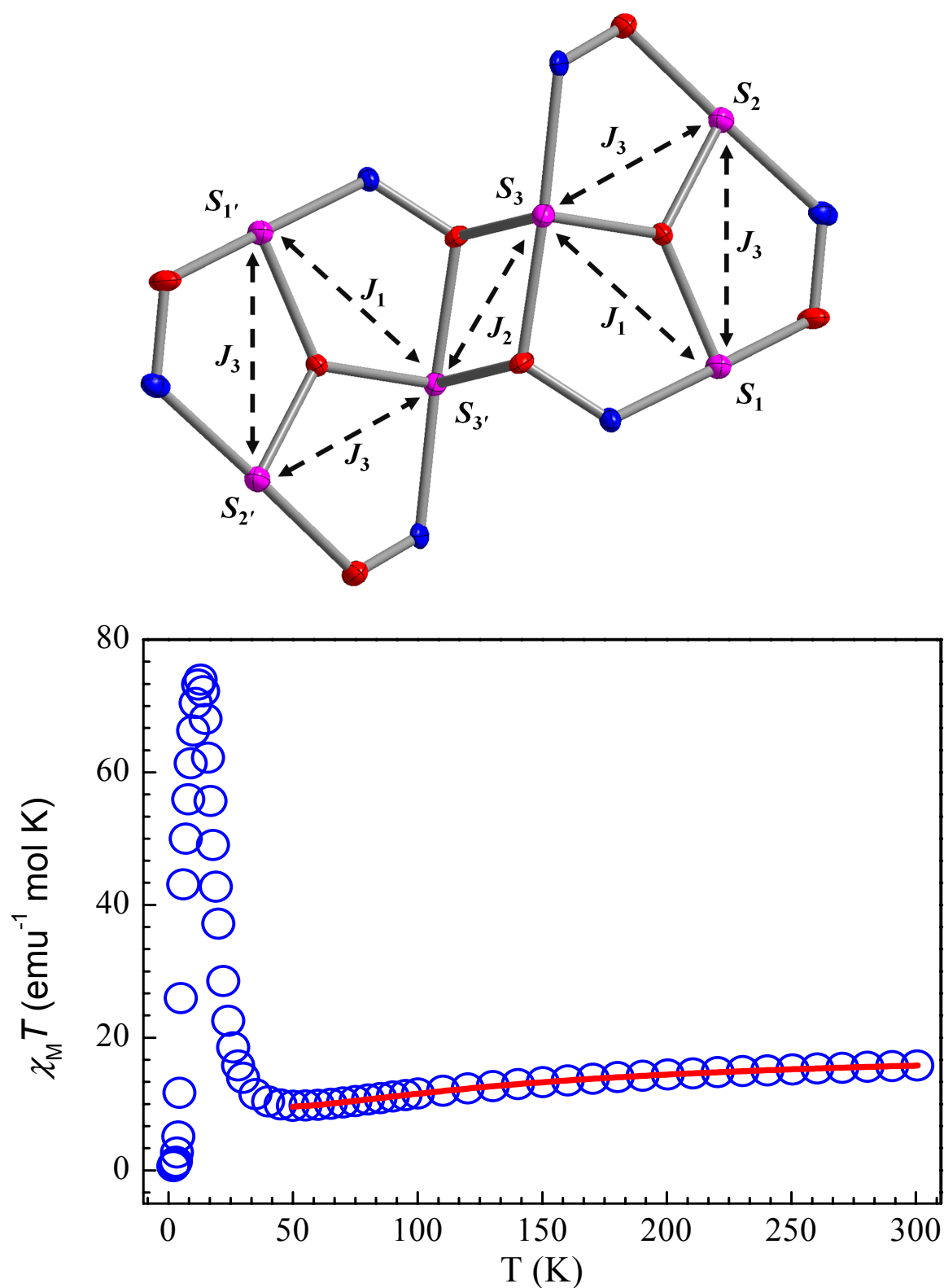
Figure 4S. Exchange pathway of manganese centers for complex **1** (top); and the plot of $\chi_M T$ versus T for complex **1** in an applied field of 1 kG from 1.8 to 300 K (bottom) with the best theoretical fit of Mn_6 core (bottom, solid line).

The three coupling constants that are strictly required and the spin Hamiltonian is given in Eq. (1):

$$H = -2J_1(S_1S_3 + S_{1'}S_{3'}) - 2J_2(S_3S_{3'}) - 2J_3(S_1S_2 + S_2S_3 + S_{1'}S_{2'} + S_{2'}S_{3'}) \qquad (1)$$

The Kambe approach for isotropic exchange-coupled systems[5] is a very useful and facile method for yielding energy eigenvalues and eigenvectors; however, entangled exchange paths sometimes prevent the splitting of a whole system into some interacting partial spin sums. An alternative approach, block diagonalization, is available for general isotropic spin systems.[5,6,7] It is based on the observation that the HDVV Hamiltonian preserves the z-component of total spin S, $S_Z = \sum_i s_Z(i)$, where $s_Z(i)$ is the z-component of spin on the i-th metal ion in a molecule, owing to the commutation relation $[\hat{H}_{\text{HDVV}}, \hat{S}_Z] = 0$. For Mn(III)$_6$ complexes, the full matrix dimension is $(2s + 1)^N = 15625$, which is not easily solved. However, the commutation relation allows us to solve each block matrix with different S_Z values separately. Thus, we can confine ourselves to an $S_Z = 0$ block matrix with only 1751 dimension, which are much fewer than those for the full matrix size. Although a more aggressive reduction of matrix size can be sometimes attempted using the topological symmetry of a molecule, S_Z block matrix diagonalization works without any symmetry restrictions and is applicable to general isotropic systems. Starting with decoupled basis vectors, $|s_Z(1), s_Z(2), s_Z(3), s_Z(4), s_Z(5), s_Z(6)\rangle$, the largest block matrix is constructed in the $S_Z = 0$ subspace for integer spin systems. (the $S_Z = -1/2$ subspace should be used for half-odd spin systems). The block matrix, being much easier to solve than the full matrix, is diagonalized to provide energy eigenvalues and eigenvectors expressed in terms of decoupled basis vectors. Invoking another commutation relation $[\hat{H}_{\text{HDVV}}, \hat{S}^2] = 0$, the square of total spin S^2 is another good quantum number, which we require for labeling an eigenstate along with S_Z. In order to obtain S, the total-spin raising operator ($\hat{S}^+ = \sum_i \hat{s}^+(i)$) is evaluated for each

eigenvector using $\langle S_Z + 1 | \hat{S}^+ | S_Z \rangle = \sqrt{(S - S_Z)(S + S_Z + 1)}$, which yields

$S = \frac{1}{2}\left(\sqrt{1 + 4\langle 1 | \hat{S}^+ | 0 \rangle^2} - 1 \right)$. For half-odd integer spin systems, $S = \langle +1/2 | \hat{S}^+ | -1/2 \rangle - \frac{1}{2}$

should be used instead.

Once the energy eigenvalues $E(S, S_Z)$ are obtained, the Van Vleck formula[8] can be used to calculate magnetic susceptibilities as a function of temperature:

$$\chi_m = \frac{N\mu_{\text{eff}}^2}{3k_{\text{B}}T}$$

$$\mu_{\text{eff}}^2 = g^2\mu_{\text{B}}^2 \sum_{\text{all } S} S(S+1)(2S+1)\exp[-E(S,S_Z)/k_{\text{B}}T] \bigg/ \sum_{\text{all } S}(2S+1)\exp[-E(S,S_Z)/k_{\text{B}}T]$$

All the procedures were coded using the IGOR Pro graphics software package,[9] which is capable of performing non-linear least-squares optimization of a model Hamiltonian.

5. C. Raghu, I. Rudra, D. Sen, S. Ramasesha, *Phys. Rev. B* **2001**, *64*, 064419.
6. N. Regnault, T. Jolicoeur, R. Sessoli, D. Gatteschi, M.Verdaguer, *Phys. Rev. B* **2002**, *66*, 054409.
7. G. Chaboussant, A. Sieber, S. Ochsenbein, H. U. Güdel, M. Murrie, A. Honecker, N. Fukushima, B. Normand, *Phys. Rev. B* **2004**, *70*, 104422.
8. R. L. Carlin, *Magnetochemistry*, Springer-Verlag, Berlin Heidelberg, **1986.**
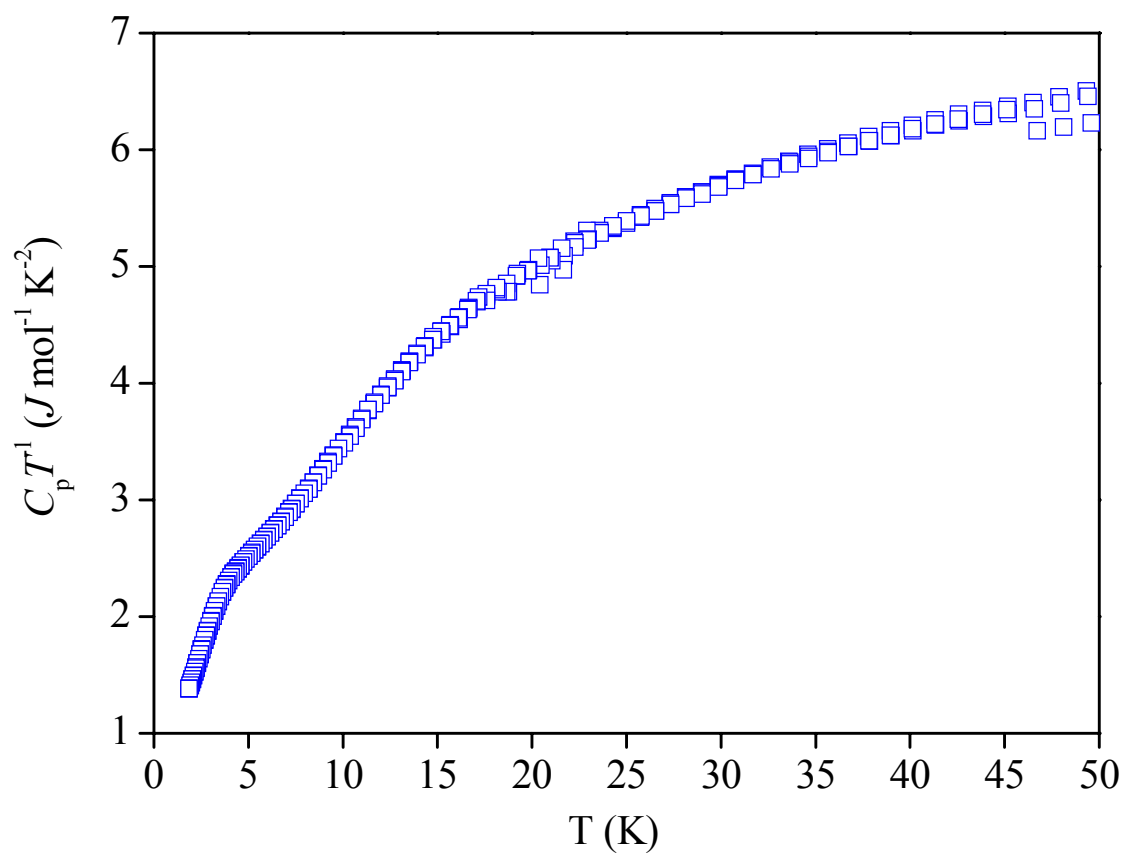9. IGOR Pro 6, WaveMetrics Inc.

Figure 5S. Plot of $C_p T^{-1}$ vs. T for a pellet piece of grounded polycrystalline of complex **1** measured under a zero applied field.
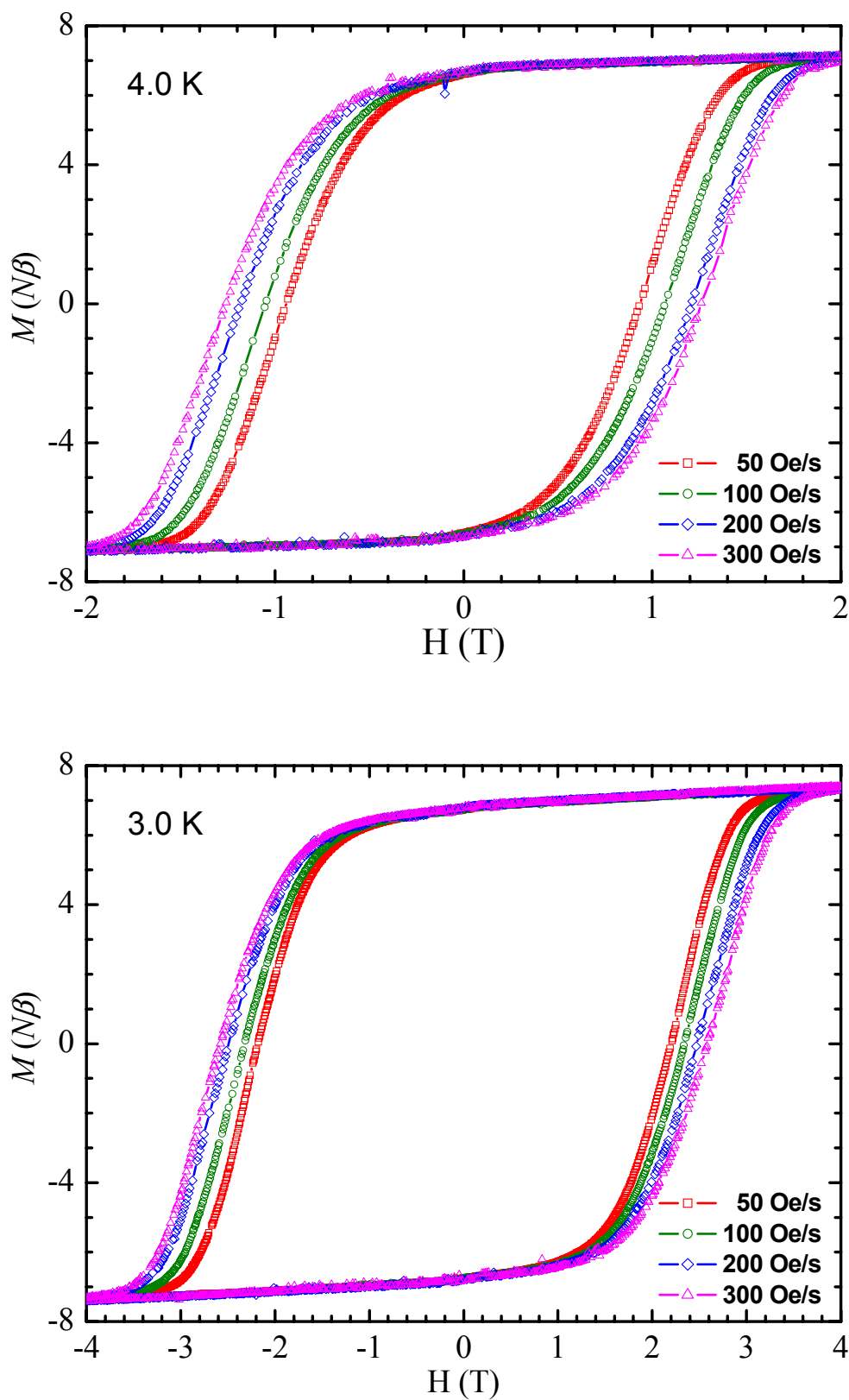
Figure 6S. Magnetization hysteresis loops for **1** for various scan rates at T = 4.0 K (top) and 3.0 K (bottom).